

On the optimal calibration of VVV photometry

Gergely Hajdu · István Dékány ·
Márcio Catelan · Eva K. Grebel

Received: date / Accepted: date

Abstract Prompted by some inconsistencies in the photometry of the VISTA Variables in the Vía Láctea (VVV) survey, we conduct a revision of the standard calibration procedure of VISTA data in the J , H , and K_S passbands. Two independent sources of bias in the photometric zero-points are identified: intra-array variations in the detector's response, and the blending of local secondary standard stars. Their combined effect on the data results in both a space-varying bias in the absolute photometric calibration, and a time-varying error in the photometric zero-points on various time-scales. The former affects studies that rely on an absolute magnitude scale, while the latter can also affect the shapes and amount of scatter in the light curves, thus potentially hampering their proper classification. We show that these errors can be effectively eliminated by relatively simple modifications of the standard calibration

G. Hajdu

Instituto de Astrofísica, Facultad de Física, Pontificia Universidad Católica de Chile,
Av. Vicuña Mackenna 4860, 7820436 Macul, Santiago, Chile
Millennium Institute of Astrophysics, Santiago, Chile
E-mail: ghajdu@astro.puc.cl

I. Dékány

Astronomisches Rechen-Institut, Zentrum für Astronomie der Universität Heidelberg,
Mönchhofstr. 12-14, 69120 Heidelberg, Germany
E-mail: idekany@uni-heidelberg.de

M. Catelan

Instituto de Astrofísica, Facultad de Física, Pontificia Universidad Católica de Chile,
Av. Vicuña Mackenna 4860, 7820436 Macul, Santiago, Chile
Millennium Institute of Astrophysics, Santiago, Chile
Centro de Astro-Ingeniería, Pontificia Universidad Católica de Chile,
Av. Vicuña Mackenna 4860, 7820436 Macul, Santiago, Chile
E-mail: mcatelan@astro.puc.cl

E. K. Grebel

Astronomisches Rechen-Institut, Zentrum für Astronomie der Universität Heidelberg,
Mönchhofstr. 12-14, 69120 Heidelberg, Germany
E-mail: grebel@ari.uni-heidelberg.de

procedure, and demonstrate the effect of the recalibration on the VVV survey’s data quality. We give recommendations for future improvements of the pipeline calibration of VISTA photometry, while also providing preliminary corrections to the VVV JHK_S observations as a temporary measure.

Keywords Photometric calibration · Near-infrared photometry · VISTA · Photometric zero points

1 Introduction

VISTA Variables in the Vía Láctea (VVV; Minniti et al., 2010) is an ESO Public Survey of the bulge and an adjoining part of the Galactic mid-plane, covering approximately 520 square degrees of the sky. It uses the Visible and Infrared Survey Telescope for Astronomy (VISTA; Sutherland et al., 2015), equipped with the VISTA IR Camera (VIRCAM). VVV acquired time-series photometry of nearly a billion point sources in the near-infrared K_S band between 2009 and 2015, and additional sparse photometry in the Z , Y , J , and H bands over its entire area. An extension of the survey called VVV eXtended (VVVX; Minniti, 2018) is currently in progress.

Standard data products for the VVV survey, as well as other ESO surveys carried out by VISTA, are produced by the VISTA Data Flow System (VDFS, Emerson et al., 2004; Irwin et al., 2004). It comprises a series of software pipelines for quality control and system monitoring by ESO, image processing, source detection, photometry and calibration by the Cambridge Astronomy Survey Unit (CASU, see Hodgkin et al., 2009; González-Fernández et al., 2018) and data curation by the VISTA Science Archive (VSA, Cross et al., 2012).

The VDFS performs photometry on two different image end products known as *pawprints* and *tiles*. A pawprint is a single detector frame stack combined from two slightly jittered VIRCAM exposures, and is thus composed of 16 sub-images, one from each of VIRCAM’s detector chips, covering a discontinuous area of the sky. At each observational *epoch*, a series of 6 pawprints are taken over a *field* with overlapping offset pointings in a ~ 3 -minute time interval, in order to fill the gaps between the detector’s chips. Consequently, most of the sources have multiple pawprint-based photometric measurements at each epoch. Pawprints are further combined into contiguous mosaic images known as *tiles*, which lead to a separate line of photometric data products. Tile-based photometry is less precise and accurate due to the complicated image processing involved in image mosaicking, but it has a slightly higher limiting magnitude. In this study, we only consider pawprint-based photometry. Both photometric data products are calibrated to local secondary standard stars from the 2-Micron All-Sky Survey (2MASS; Skrutskie et al., 2006). For a more comprehensive technical description of the data processing by CASU, we refer to González-Fernández et al. (2018, and references therein). Standard data products from CASU are considered to be science-ready and serve as direct input for the VSA.

The VVV survey’s standard data products, as provided by CASU, already formed the basis of hundreds of scientific publications in diverse interlinked astronomical fields, ranging from studies of the stellar populations of the Galactic bulge (e.g., Gonzalez et al., 2012; Dékány et al., 2013; Wegg, & Gerhard, 2013), to analyses of interstellar extinction (Gonzalez et al., 2012; Schultheis et al., 2014; Nataf et al., 2016) and the census and characterization of stellar clusters in the Milky Way (Borissova et al., 2011; Chené et al., 2012; Alonso-García et al., 2015), to mention only a few. Most of these studies concern objects located toward crowded stellar fields at low Galactic latitudes highly reddened by interstellar dust, where VVV has a unique advantage over optical surveys. The accuracy of the absolute calibration of VVV photometry under such adverse observational conditions is of critical importance for the astrophysical characterization of these objects.

Evidence has been accumulating that the standard photometric data products of the VVV survey show significant anomalies. In this study, we review the pipeline calibration procedure of VISTA photometry by the VDFS, revealing that the photometric zero-points in the J , H , K_s bands are affected by significant time-varying biases that can adversely affect scientific conclusions, and that can be largely eliminated by further optimization of the calibration method.

2 Inconsistencies in the VVV photometry

During our study of the RR Lyrae stars along the southern Galactic mid-plane (Dékány et al., 2018), a fraction of our sample showed large inconsistencies between individual H -band measurements. Fig. 1 shows concrete examples of this for two different stars: on the left panel, the H -band measurements of the star come from two separate pawprints at the same epoch, while on the right panel the H -band data come from two different nights. In both cases, the two H -band measurements are inconsistent with the predicted light variation (Hajdu et al., 2018). In the study of Dékány et al. (2018), J -band measurements did not show such an anomaly, and they were available for almost all RR Lyrae stars in our sample, enabling us to estimate their reddening. However, many objects in the VVV survey, such as distant Cepheids, are extremely obscured by interstellar dust, preventing their detection in the J band. As a result, H -band observations play a crucial role in the characterization of distant, heavily reddened VVV sources. Thus, understanding the cause of the H -band photometric inconsistencies and making the necessary corrections is essential.

An additional source of systematic bias in the VDFS photometry was discovered by Jurcsik et al. (2018) during their study of the Blazhko effect in the near-infrared. They note that part of their VVV K_s -band RR Lyrae light curves showed systematic offsets between measurements corresponding to different pawprints and/or overlapping fields. These offsets were manually cor-

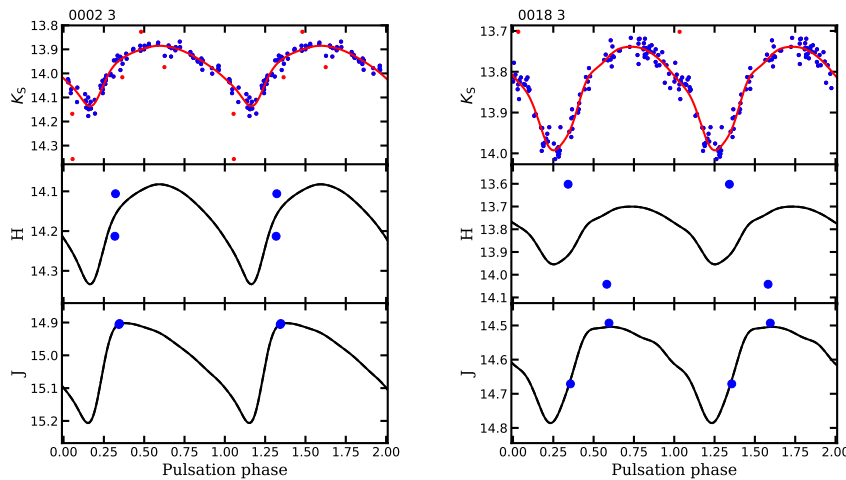


Fig. 1 Phase-diagrams of two RR Lyrae stars from Dékány et al. (2018) showing their J , H , K_s photometry from the VVV survey. The red curves show light curve models fitted directly to the K_s data, while the black curves are light variations predicted by the `PyFiNeR` routine of Hajdu et al. (2018). Note the inconsistent H -band measurements (middle panels) for both objects.

rected by Jurcsik et al. (2018) on a relative scale, but this additional source of scatter also warrants a revision of the VISTA photometry in all passbands.

3 The calibration of VISTA to 2MASS

The standard procedure of photometric calibration of VISTA data is based on the software pipeline by Hodgkin et al. (2009), developed for the Wide Field Camera (WFCAM; Casali et al., 2007) of the United Kingdom Infrared Telescope (UKIRT) on Mauna Kea, Hawai’i. CASU have provided multiple versions of the photometry, differentiated by version numbers. At the time of this writing, version 1.3 has been completed for the entire VVV data set and version 1.5 is being prepared. Versions 1.3 and 1.5 share the procedures of source extraction and photometry, and only differ in the conversion formulae involved in the absolute calibration (González-Fernández et al., 2018).

The VISTA instrumental magnitudes are calibrated to the common VISTA photometric system on a pawprint basis by applying a zero-point shift to match the magnitudes of an ensemble of local secondary standard stars from the 2MASS survey, converted to the VISTA system. Changes in the individual detector sensitivities are accounted for by an additional offset, calculated on a monthly basis for every filter.

In order to investigate the previously discussed photometric anomalies, we retrieved the photometry provided in the 2MASS Point Source Catalog

(Skrutskie et al., 2006) from the Infrared Processing & Analysis Center¹ for all stellar sources in the following areas:

$$\begin{aligned} \text{bulge: } & -10.4^\circ < l < 11^\circ ; -10.5^\circ < b < 5.3^\circ \\ \text{disk: } & -65.5^\circ < l < -9^\circ ; -2.4^\circ < b < 2.4^\circ. \end{aligned}$$

These two data sets completely encompass the bulge and disk footprints of the VVV survey, and contain approximately 13.7 and 10.6 million stars, respectively.

Version 1.3 of the CASU photometry uses the following transformation equations between the 2MASS and the VISTA systems (González-Fernández et al., 2018):

$$J_{\text{VISTA},1.3} = J_{2\text{MASS}} - 0.077 \times (J - H)_{2\text{MASS}} + 0.010 \times E(B - V) \quad (1)$$

$$H_{\text{VISTA},1.3} = H_{2\text{MASS}} + 0.032 \times (J - H)_{2\text{MASS}} + 0.015 \times E(B - V) \quad (2)$$

$$K_{\text{SVISTA},1.3} = K_{S2\text{MASS}} + 0.010 \times (J - K_S)_{2\text{MASS}} + 0.005 \times E(B - V); \quad (3)$$

while their version 1.5 uses the following equations:

$$J_{\text{VISTA},1.5} = J_{2\text{MASS}} - 0.031 \times (J - K_S)_{2\text{MASS}} + 0 \times E(B - V) \quad (4)$$

$$H_{\text{VISTA},1.5} = H_{2\text{MASS}} + 0.015 \times (J - K_S)_{2\text{MASS}} + 0 \times E(B - V) \quad (5)$$

$$K_{\text{SVISTA},1.5} = K_{S2\text{MASS}} - 0.006 \times (J - K_S)_{2\text{MASS}} + 0.005 \times E(B - V). \quad (6)$$

The color excess $E(B - V)$ towards each star is estimated in multiple steps (González-Fernández et al., 2018). First, the map of $E(B - V)$ calculated from the infrared emission of dust by Schlegel et al. (1998) is interpolated to the coordinates of each 2MASS source. The $E(B - V)$ values above 0.1 are modified as:

$$E'(B - V) = 0.1 + 0.65 \times (E(B - V) - 0.1), \quad (7)$$

following the correction introduced by Bonifacio et al. (2000)². Likewise, as integrated extinction maps can overestimate the extinction of individual stars, further corrections are applied for each star according to Sect. 4.4 of González-Fernández et al. (2018). These final $E(B - V)$ values are used for the magnitude conversion of 2MASS sources via Eqs. 1–6 for both the bulge and the disk area.

González-Fernández et al. (2018) note that there are small magnitude zero-point offsets between versions 1.3 and 1.5 of VISTA photometry, mainly caused by the change in the transformation Eqs. 1–6. Our conversion of the 2MASS

¹ www.ipac.caltech.edu

² Note that, for version 1.5, González-Fernández et al. (2018) use unmodified Schlegel et al. (1998) $E(B - V)$ values. Only the K_S band is marginally affected by this, where the difference between the two approaches causes an offset of ~ 0.001 magnitudes.

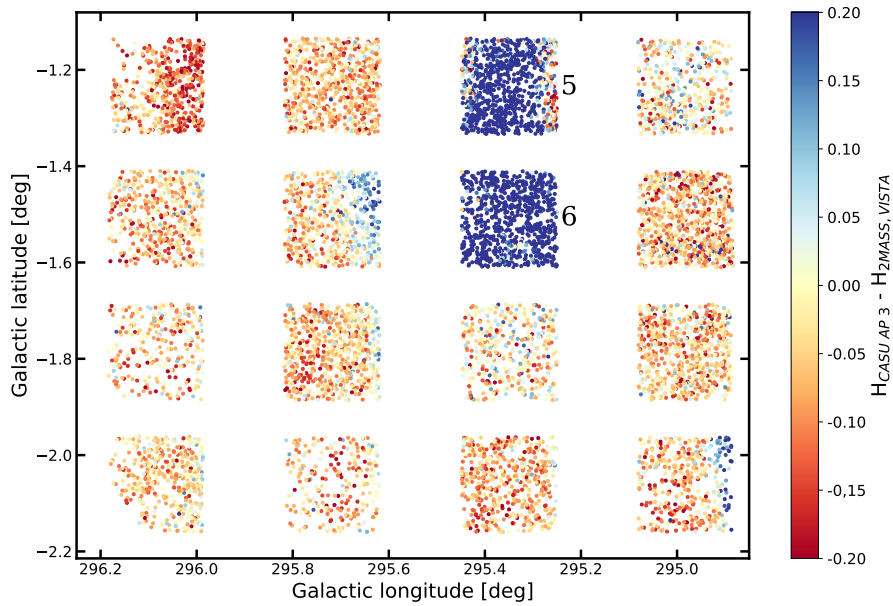


Fig. 2 Photometric difference between VISTA H -band observations and converted 2MASS magnitudes for one pawprint. Chips 5 and 6 (marked on the figure by numbers) possess systematically fainter magnitudes than all other detectors. Furthermore, some intrachip differences are also evident when comparing the two sources of photometry.

photometry to the versions 1.3 and 1.5 of the VISTA system show differences consistent with the ones found by González-Fernández et al. (2018, see their Eqs. C9–C11), validating our analysis³.

4 Revision of the H -band VVV photometry

The converted 2MASS magnitudes obtained in Sect. 3 allow an independent check of the photometry delivered by the VDFS. Fig. 2 shows the differences between the converted 2MASS H -band magnitudes of stellar sources and their VISTA photometry as provided by CASU, in one particular pawprint of the low source density VVV field *d001* (see Minniti et al. 2010 for field definitions). It is immediately apparent that the joint magnitude zero-point calibration of the entire pawprint causes underestimated magnitudes on chips 5 and 6, and generally overestimated magnitudes in the rest of the chips. The distribution of magnitude differences even show small-scale systematic variations within some of the chips.

³ González-Fernández et al. (2018) calculate these differences on calibrated VISTA photometry over different sky regions, while here this was done for the converted 2MASS magnitudes only in the VVV sky footprint. Hence, these differences are not expected to be exactly the same, owing to the different sky areas covered by stars of the two samples, as well as the extinction terms in Eqs. 1–6.

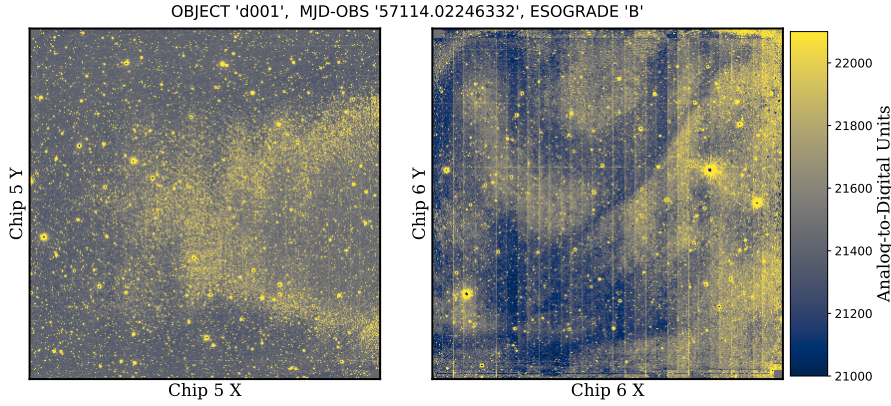


Fig. 3 The H -band (calibrated) images of chips 5 and 6 (marked by numbers), corresponding to the photometric difference map presented in Fig. 2. Both chips suffer from dark regions with diminished point-source analog-to-digital unit counts. The high background counts indicate suboptimal observing conditions.

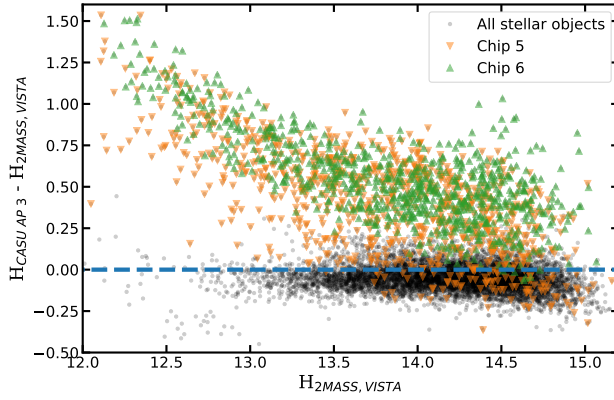


Fig. 4 H -band magnitude differences between the VVV photometry calibrated by CASU and the corresponding converted 2MASS measurements for the same pawprint as in Figs. 2 and 3. The non-linear response of the VIRCAM chips 5 and 6 results in lower source counts and biased photometry for these detectors. Furthermore, while the photometry from the other detectors is mostly internally consistent, the pawprint-wise zero-point calibration scheme employed by CASU results in a systematic overestimation of the point-source magnitudes.

The original, reduced H -band VISTA images from chips 5 and 6 are shown in Fig. 3. Both images exhibit very apparent artifacts, probably caused by the non-linearity of these two chips when the “sky background” (i.e., the atmospheric foreground flux) is high. The straight lines across chip 6 possibly originate from imperfections in the detector’s manufacturing process.

The distribution of H -band magnitude differences for the same pawprint of field *d001* are shown in Fig. 4. In accordance with Fig. 2, the magnitudes in chips 5 and 6 are underestimated, while they are generally overestimated

on all other chips. Magnitudes measured in chips 5 and 6 also show large dispersion and non-linearity. In contrast, the magnitudes from the other chips show small dispersions and no apparent non-linearity under the same sky conditions. Therefore, photometric measurements obtained with these chips in the H -band should generally be reliable after a chip-wise zero-point correction. Meanwhile, H -band photometry acquired by chips 5 and 6 under suboptimal conditions should generally be treated as suspect. Indeed, the same behavior of the VIRCAM detectors can frequently be observed for other fields during the entire timespan of the VVV survey.

It has to be noted that similar offsets, apparently caused by unfavorable observing conditions, were not found in the case of the J and K_S photometry, as the atmospheric flux in those bands is generally lower.

5 VVV magnitude zero-point bias in dense stellar fields

The converted 2MASS photometry from Sect. 3 allows a general revision of the VISTA photometry for all filters. In the following, we investigate the effect of source crowding on the photometric calibration of VVV data in the J , H , and K_S bands.

Aside from the area toward the nuclear bulge, one of the fields with the highest source density is *b307*, due to its position toward Baade’s Window. The top and bottom panels of Fig. 5 compare the VDFS-calibrated VVV magnitudes of stellar sources and the corresponding converted 2MASS measurements for the H and J bands, respectively, for all stellar sources from a single paw-print of field *b307*. Most of the fainter stars (2MASS magnitude $\gtrsim 12$) are offset from the fiducial line. Furthermore, most outliers from the main locus have positive deviations, meaning that the same sources appear systematically dimmer in the CASU source catalog with respect to 2MASS. Visual inspection of images taken by both instruments revealed that almost all of the latter stars are blended in the 2MASS observations, while typically being resolved into 2–4 separate point sources by VISTA. Examples of severe, medium and insignificant blending in the 2MASS observations are shown in Fig. 6, for the individually marked sources in the bottom panel of Fig. 5.

CASU’s calibration pipeline calculates the zero-points of individual paw-prints as the mean difference between the instrumental magnitudes of point sources and their converted 2MASS counterparts. In fields of high stellar density, several VISTA sources can be blended into one 2MASS source. The positional cross-matching procedure of CASU does not take this effect properly into account by allowing loose tolerances, leading to the photometric zero-point bias revealed here. Fig. 7 illustrates the size and spatial dependence of this bias, showing the change in magnitude zero-points as measured by the CASU pipeline during ~ 4 hours of VISTA observations of VVV fields. For comparison, the variation in the atmospheric seeing measured on the K_S -band observations is also shown. These two quantities are clearly not correlated with each other. During this particular night, VISTA was acquiring multi-band ob-

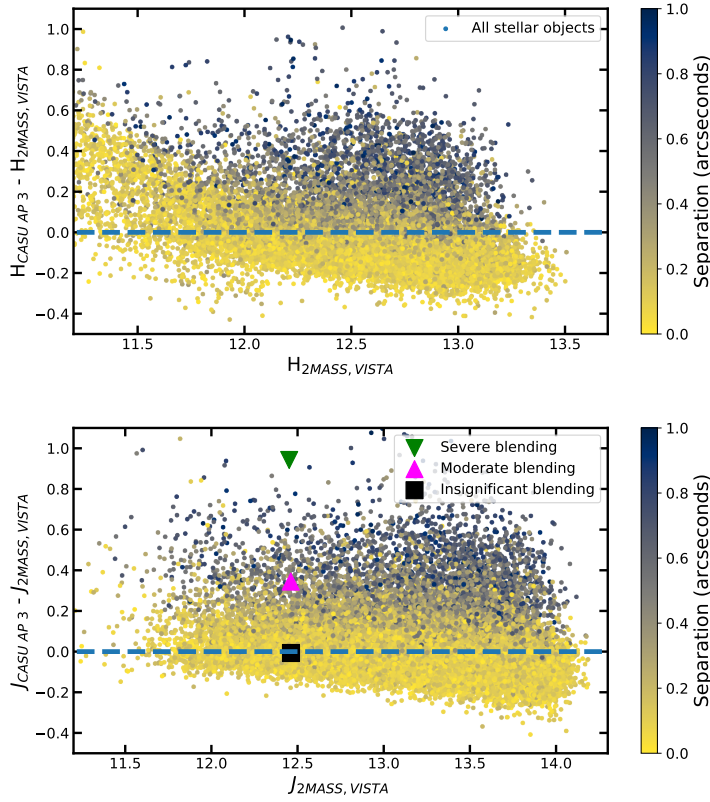


Fig. 5 H and J -band photometric bias in the VVV field $b307$. *Top*: H -band magnitude differences in field $b307$ between the converted 2MASS measurements and the VVV aperture photometry of stellar sources calibrated by CASU. Note the systematic offset from the fiducial line for the majority of sources with 2MASS magnitudes fainter than ~ 12 mag. The color scale denotes the separation between the coordinates of the sources in the 2MASS and VISTA catalogs. *Bottom*: The same as in the top panel, but for the J band. The 2MASS and VISTA images of the three individually marked stars are shown in Fig. 6.

servations for the VVV survey, hence the availability of all three of the bands J , H , and K_S . Near the beginning and the end of this night, images were taken in uncrowded fields far from the Galactic plane, while during the middle of the night, the densest VVV tiles were observed. As can easily be seen, the amplitude of the photometric zero-point bias also depends on the passband due to the different blending levels at different wavelengths. The H -band measurements suffer from the largest bias. Besides low stellar densities, high extinction can also reduce the size of this bias by diminishing the detection rate of faint 2MASS sources.

CASU also provide photometric catalogs for tile images, resulting from the combinations of six pawprints acquired at the same epoch. González-Fernández et al. (2018) describe a grouting process for the correction of tile-based pho-

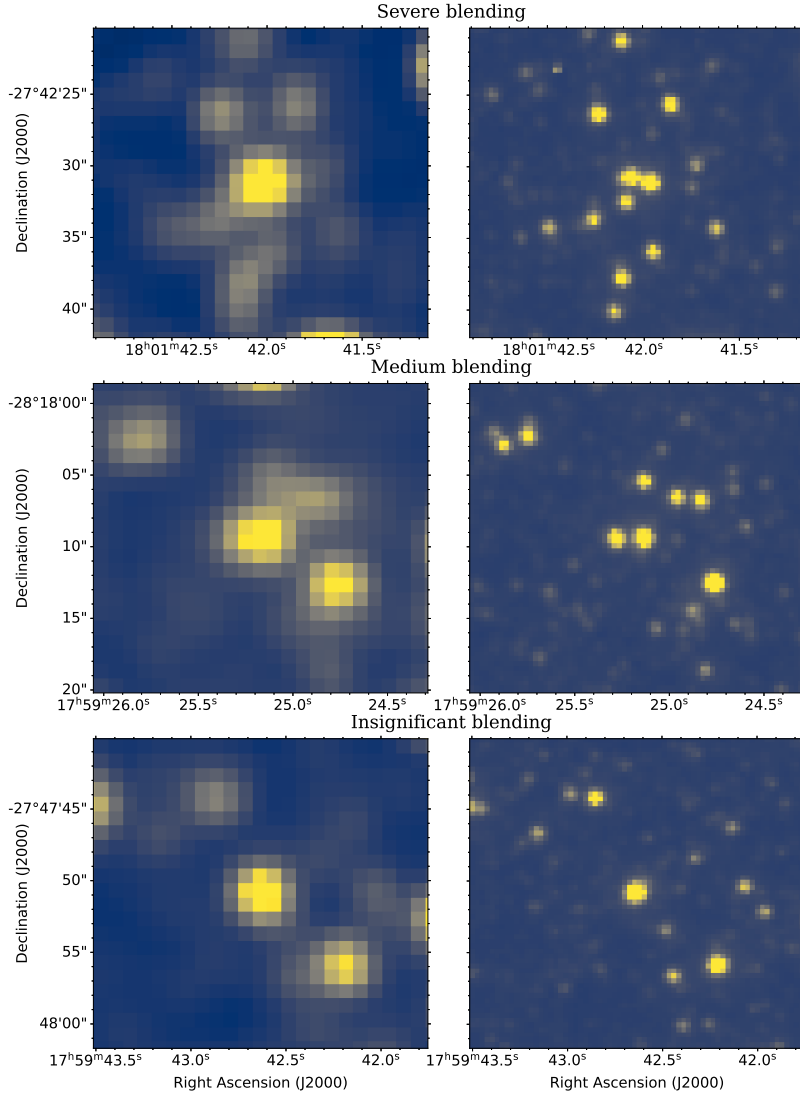


Fig. 6 Examples of severe, medium, and insignificant point-source blending in the 2MASS *J*-band observations in the area of the VVV survey, shown by the top, middle, and bottom panels, respectively. The sources in the image centers correspond to the objects marked by various symbols in the bottom panel of Fig. 5. *Left*: *J*-band images of the 2MASS observations. *Right*: *J*-band VISTA images of the same fields.

tometry, whereby they take into account the photometric zero-point offsets between individual pawprints of a tile, among other effects. They attribute these offsets to variations in the atmospheric extinction. However, we stress that varying levels of zero-point calibration bias due to blending also come into play in generating such offsets within a single observational epoch. Each paw-

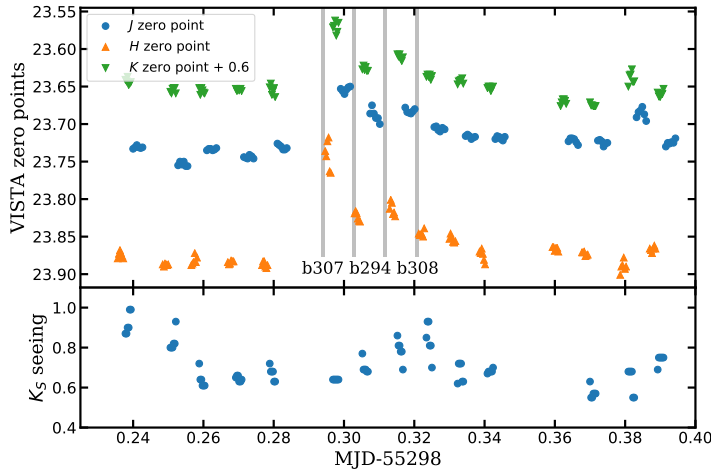


Fig. 7 *Top:* Evolution of the VIRCAM@VISTA zero-points as calculated by the CASU pipeline during a period of 4.2 hours of one night. Zero-points in tiles with high stellar density (especially tiles *b307*, *b294*, and *b308*, marked by the vertical grey bars as well as text) are systematically underestimated due to the photometric blending in the 2MASS catalog. *Bottom:* The seeing measured on the K_S -band observations. The changes in seeing and zero-points are not correlated.

print of a tile covers a slightly different subregion of a field due to their pointing offsets. If the distribution of interstellar extinction significantly differs between these subregions, then the amount of crowding, and hence the blending in the 2MASS catalog, will vary between pawprints. As blending biases the pawprint zero-points, varying levels of blending between VISTA pawprints increase the scatter of zero-points measured by the CASU pipeline, providing an additional source of pawprint-to-pawprint variation, measured and partially corrected in the grouting process. This effect can be seen in Fig. 7 as an increased scatter in the pawprint zero-points for fields with high stellar density.

6 Recalibration of the JHK_S observations in the VVV survey

As the photometric biases detailed in Sects. 4 and 5 mostly manifest themselves in the zero-points of the VIRCAM detectors and the VISTA pawprint observations, respectively, they can mostly be corrected for by a revision of the per-detector zero-points.

The zero-point calculation procedure of González-Fernández et al. (2018) allows a relatively large, 1 arcsecond cross-match radius of tolerance between positions in the 2MASS catalog and the VVV source catalogs. The color scale in Fig. 5 shows the angular separation between the VVV sources and their cross-matched 2MASS equivalents. Most notably, the 2MASS stellar sources lying above the fiducial lines (hence probably being blends in the 2MASS catalog) generally have higher separations than those belonging to the main

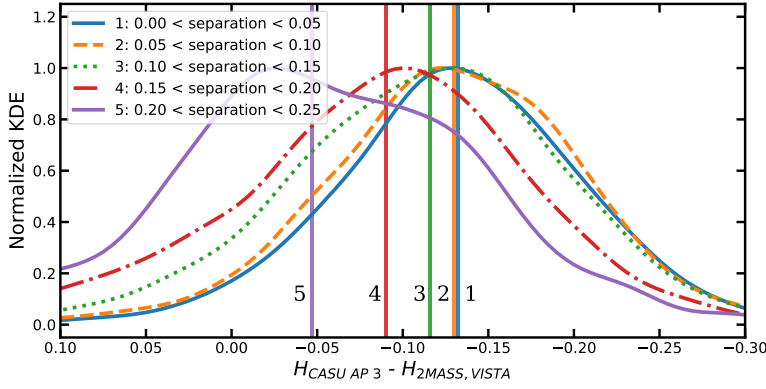


Fig. 8 Kernel density estimates (KDEs) of magnitude differences in different cross-match angular separation bins in the H -band in VVV tile $b307$ (top panel of Fig. 5, for stars fainter than 12.5 magnitudes in the 2MASS catalog). Different curves correspond to different matching distances, as indicated in the inset (in arcsec). The KDEs are normalized to their individual maxima. Vertical bars mark the median values of different bins. Note the progressively fainter magnitudes measured by VISTA with increasing cross-match radius.

locus of unblended stars. Naturally, as many sources are blended in the 2MASS Point Source Catalog towards fields with high stellar density, not only their magnitudes, but also their measured positions are affected by the blending, which explains the increased positional errors.

The dependence of the bias on the cross-match radius is further examined in Fig. 8 for the same H -band pawprint of the VVV field $b307$, shown previously on the top panel of Fig. 5. It can be seen that for higher angular separations, the VVV magnitudes become progressively fainter due to the increasing fraction of blending in the 2MASS catalog with increasing tolerance in the cross-matching. With a tolerance of 0.1 arcseconds, the effect of blending becomes minimal, as shown by the median values of the samples, marked by vertical bars.

We developed a method for correcting the magnitude zero-points of individual detectors, taking into account the specific properties of the VVV survey’s observations. The calibration process described by González-Fernández et al. (2018) calculates zero-points on the pawprint level. The principal reason for this is to guarantee that enough 2MASS stars are available for the robust determination of zero-points, even in high Galactic latitude fields. As VVV fields are generally rich in stars, we calculate the zero-point corrections for each detector chip separately in each pawprint of each epoch for the five smallest apertures. The main points of this correction method are the following:

- The 2MASS Point Source Catalog converted to the VISTA version 1.5 system (Sect. 3) is used as the source catalog for the (re)calibration of VVV observations. As in some cases non-linearity affects VISTA observations down to 12.5 magnitudes (see upper panel of Fig. 5), only observations fainter than this limit are used.

Table 1 Individual photometric zero-point correction factors for each observation, detector, and aperture in the VVV survey. This table is available in its entirety in machine-readable form as Electronic Supplementary Material of the journal.

Field	OBS ^a	Band	Chip	ZPT ^b	Aperture ^c					σ_{tot} ^d					Nstars ^e
					1	2	3	4	5	1	2	3	4	5	
d001	v20100314_00245	J	1	23.702	-0.011	-0.012	-0.011	-0.013	-0.017	0.053	0.046	0.043	0.044	0.052	585
d001	v20100314_00245	J	2	23.699	+0.008	+0.007	+0.006	+0.002	-0.003	0.055	0.055	0.051	0.050	0.052	834
...
d001	v20100314_00221	H	1	23.848	+0.009	+0.014	+0.014	+0.013	+0.007	0.061	0.056	0.048	0.048	0.057	497
d001	v20100314_00221	H	1	23.850	+0.031	+0.033	+0.031	+0.028	+0.024	0.060	0.052	0.050	0.049	0.056	787
...
d001	v20100129_00205	K _S	1	22.913	+0.009	+0.012	+0.013	+0.015	+0.021	0.076	0.063	0.062	0.058	0.066	470
d001	v20100129_00205	K _S	2	22.907	+0.021	+0.024	+0.029	+0.032	+0.039	0.068	0.063	0.059	0.060	0.063	651
...

^a Identifier of the VISTA pawprint.

^b Value of the magnitude zero-point header keyword MAGZPT in the CASU v1.3 files.

^c Magnitude zero-point corrections for the five smallest apertures, calculated from the median difference.

^d Standard deviation calculated from the median absolute deviation (in mag units), of the VISTA-2MASS measurements (i.e., $\text{MAD} \times 1.4826$).

^e Number of VISTA-2MASS stars used to calculate the photometric offsets.

- Unified source catalogs of each VVV field are created using the procedure of Dékány et al. (2018). They are cross-matched with the converted 2MASS catalog with a tolerance of 0.15 arcseconds. The small cross-match radius helps in diminishing the effect of the photometric bias due to the different blending characteristics between the 2MASS and VISTA observations (see Sect. 5). Although this effect becomes non-marginal for cross-match radii larger than 0.1 arcseconds, it remains fairly small until 0.15 arcseconds (see Fig. 8), and the increased source counts help in deriving a more robust zero-point correction in tiles with lower stellar densities.
- The zero-point correction is calculated for each detector and each aperture of each pawprint observation as the median difference between the magnitudes of stellar sources and their corresponding converted 2MASS magnitudes. The median difference is preferred over the mean, as it is a more robust statistic in the presence of outliers (for example, variable stars).
- Individual light curves are corrected for the VISTA zero-point biases by subtracting the appropriate zero-point corrections from their original CASU magnitudes, on a frame-by-frame basis.

The format of the correction offsets, calculated for every combination of pawprint observations, VIRCAM detectors, and the five smallest apertures provided by CASU, for the *JHK_S* observations in the VVV survey, are shown in Table 1.

7 Effects of the recalibration

After calculating the photometric zero-point corrections as described in Sect. 6, the full effect of the zero-point biases described in Sects. 4 and 5 can be evaluated. Fig. 9 illustrates the effect of our recalibration on the light curves of four Cepheid variables. In the case of three Cepheids from the moderately crowded tile *b319*, their mean brightnesses in the *K_S* band have decreased by about 0.1 magnitudes. Furthermore, the scatter in their light curves decreased

by about one order of magnitude. The fourth Cepheid illustrates the mostly constant photometric offsets between different chips in the case of a VVV disk tile, which also contributes to the light curve scatter. The fact that the quality of the light curves has improved so drastically validates the choice of the chip-based recalibration of the photometric zero-points.

The spatial distribution of the magnitude offsets is affected by the pawprint pattern, as well as by the apparent temporal variation of the zero-point bias, most probably due to changes in the observing conditions and variations in telescope pointing. The decreased scatter of the light curves shown in Fig. 9 is a result of correcting for these effects. However, it is also necessary to visualize the effect of the zero-point bias on the VISTA photometry over small spatial scales.

We have constructed a uniform grid in Galactic coordinates, with grid-points separated by 0.1° in both longitude and latitude, covering the entire bulge area of the VVV survey. For each of the gridpoints, all sources within a cross-match radius of $5''$ were identified in the unified source catalogs (Sect. 6). These allowed us to determine which of the VIRCAM chips fell onto each of the gridpoints, along with the timings of the observations. In turn, this information allowed the identification of the magnitude offset corrections (calculated in Sect. 6) which contribute to the magnitude differences at each of these coordinates. The spatial distribution of the median values of the corrections in the J , H , and K_S bands across the bulge area are shown in Fig. 10. Likewise, the biases in their color indices are shown in Fig. 11. In the outer regions of the bulge, the magnitude and color differences are minimal, due to the minimal blending of VISTA calibrator stars in the 2MASS catalog. The small systematic differences in each band, seen towards the outer regions of the Galactic bulge, are caused by the systematic difference between the VISTA version 1.3 and 1.5 photometric systems. On the other hand, toward regions of high stellar density such as Baade’s Window at $l, b \sim 2.5^\circ, -2.5^\circ$, the difference increases drastically. It has to be noted that this difference behaves markedly differently from one filter to the next, most probably due to the different intrinsic colors and amount of extinction that each star in the converted 2MASS catalog (Sect. 3) is subject to. The diagonal streaks, mostly seen in the J band across the southern side of the bulge, are artifacts following the 2MASS scanning pattern and point toward zero-point offsets on the order of 0.01 mag in those regions. These artifacts appear because while we computed the photometric zero-point offsets individually for each chip, in the original CASU photometry, the zero points were determined by per pawprint, thus they are averaged over these areas.

8 Conclusions and recommendations for the future usage of VISTA observations

We have shown that the standard photometric source catalogs of the VVV survey produced by the VDFS suffer from space- and time-varying zero-point

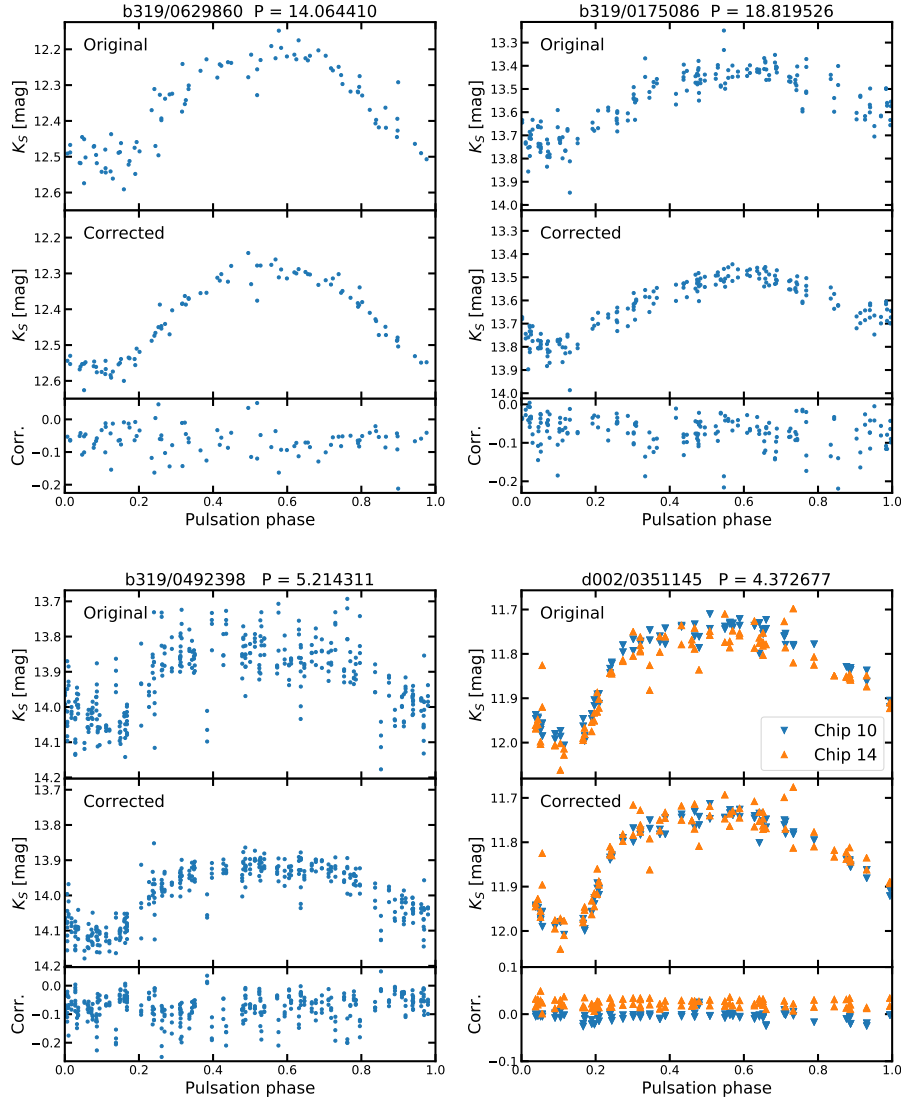


Fig. 9 K_S -band light curves of Cepheids, before and after correction for the zero-point bias with the method described in Sect. 6. *Top panels:* The original phase-folded light curves. *Middle panels:* The corrected phase-folded light curves. The magnitude scales are the same as in the corresponding *top* panels. *Bottom panels:* The offsets for individual photometric measurements. Note that the last Cepheid has VVV observations from two different VIRCAM detector chips.

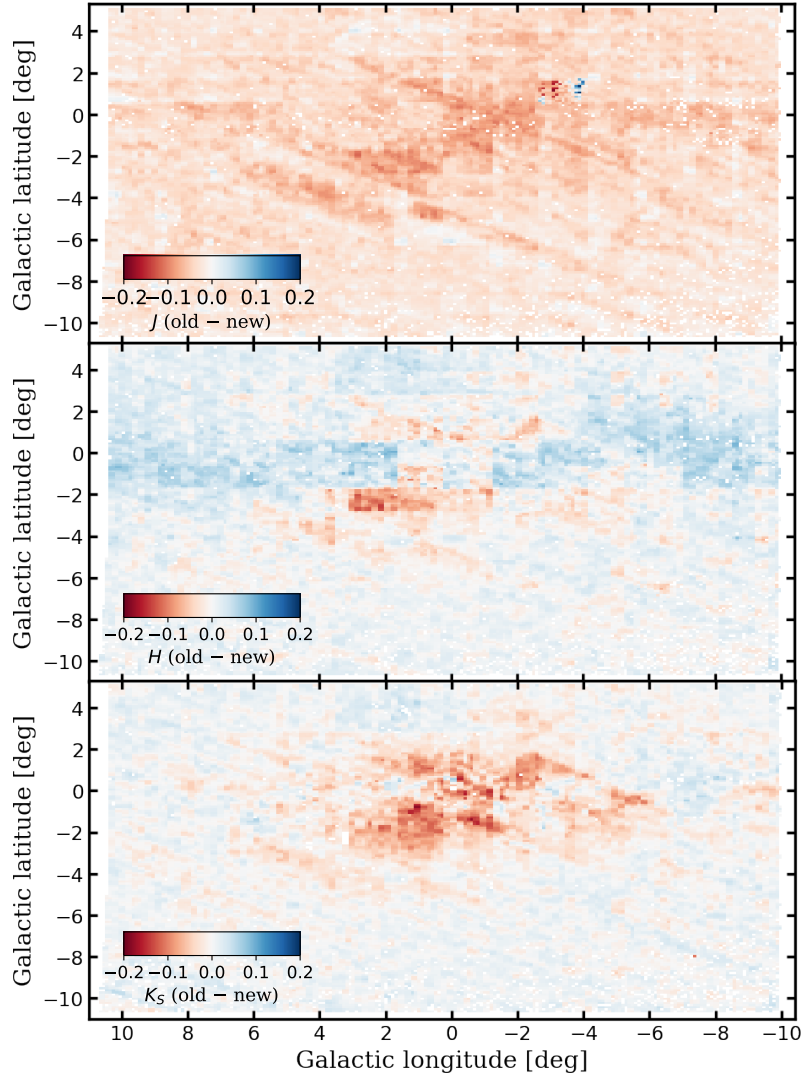


Fig. 10 Top to bottom: J , H , and K_S -band maps of the median photometric bias over the complete VVV survey bulge area.

biases. For this reason, some of the results based on VVV (and, more generally, VISTA) observations will probably need to be revised, in order to be placed on a firmer footing. For example, studies of the extinction law would likely benefit from a revision, since both the derived apparent magnitudes and colors vary towards different regions of the Galactic bulge (Figs. 10 and 11). For example, Nataf et al. (2016) studied the spatial variation of the extinction law based on combined VVV JHK_S and OGLE-IV VI photometry by tracing the changes in the color excesses of the red clump stars across the bulge. Although they

measured stellar magnitudes by a custom point-spread function (PSF) fitting photometry, their zero-point calibration is based on the CASU photometric catalogs, and thus their data likely inherit the spatial zero-point bias structure shown in Fig. 10. Nataf et al. (2016) found pairs of sight-lines where the respective red clumps occupy the same position on the K_S vs $V - I$ color-magnitude diagram, yet have very different $J - K_S$ colors (their Figs. 5 and 6). Based in part on this, they concluded that the extinction curve has a non-standard shape towards the Galactic bulge. As the compared fields are not on the same VVV pawprint or even tile, their J and K_S magnitude zero-points, and thus every color index derived from these quantities is likely affected by the zero-point bias in different ways. Studies of the nature, shape, and spatial variations of the extinction law would thus likely benefit from a deeper reexamination of the VVV photometry.

In this sense, the relatively simple recalibration procedure described in Sect. 6, and provided in Table 1, should serve only as a temporary measure in future studies utilizing VISTA observations. The selection of non-blending 2MASS stars based on their cross-match radius that we adopted is a very preliminary approach, as it still leaves a considerable fraction of blended stars in the sample for certain fields that is used for computing the zero-point corrections. Ideally, each and every 2MASS star used in the zero-point calibration of VISTA observations should be revised and potentially discarded if the VISTA observations reveal close companions within the 2MASS PSF.

Particularly in the most crowded VVV fields, PSF photometry has already proven its great value in generating deep color-magnitude diagrams and enabling time-series studies, even of faint sources (e.g., Alonso-García et al., 2018; Contreras Ramos et al., 2018; Braga et al., 2019). For PSF photometry, the light-curve scatter caused by the varying offsets between individual epochs (see the difference in scatter between corrected and uncorrected light-curves in Fig. 9) is expected to be minimized, if the data are calibrated to a single epoch of CASU aperture photometry. However, the spatially varying zero-point offsets shown in Fig. 10 might be expected to directly propagate into the zero points of the PSF photometry if said catalogs are used to derive them (as commonly done). As an alternative, a custom calibration based on the converted 2MASS photometry can be recommended for the zero-point calibration of PSF measurements, together with implementing additional steps for rejecting blended stars in the 2MASS catalog. Towards the Galactic center, PSF photometry has the unique power of resolving individual stellar sources in the VVV survey. The centermost tiles are generally observed right after and/or before more outlying tiles. Therefore, the zero-points derived for these flanking tiles could be adopted as the zero-points for the photometry of Galactic center tiles.

Alternatively, the photometric catalogs of different tiles and pawprints could be used in an “*Ubercal*”-like calibration scheme (Schlafly et al., 2012; Magnier et al., 2013). However, the photometric zero-points will have to be derived with extreme care towards regions of high stellar densities.

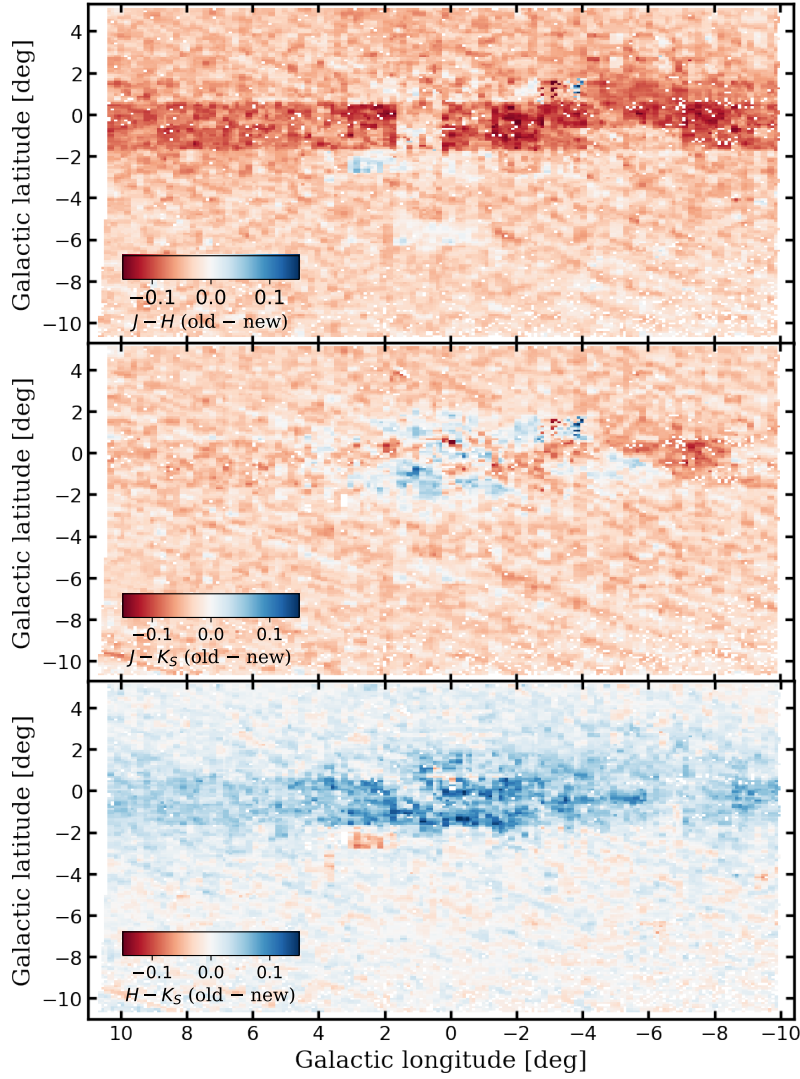


Fig. 11 As in Fig. 10, but the three panels from top to bottom show the median $J - H$, $J - K_s$ and $H - K_s$ color differences, respectively.

The VISTA photometric pipeline described by González-Fernández et al. (2018) is based on that of WFCAM (Hodgkin et al., 2009). As the resolution of the two cameras and telescope systems are quite similar, it is conceivable that observations calibrated by CASU for the latter are also affected by the photometric zero-point bias described in Sect. 5 for VIRCAM. Therefore, the recommendations described here may also be applicable to WFCAM for observations in regions of high stellar density. Furthermore, it has to be noted that VISTA observations obtained for surveys of high source-density regions,

such as the VISTA Magellanic Cloud Survey (VMC, Cioni et al. 2011), might be similarly affected by zero-point offsets caused by blending in the 2MASS catalog.

Acknowledgements G.H. and M.C. gratefully acknowledge the support provided by FONDECYT through grant #1171273; by the Ministry for the Economy, Development, and Tourism’s Millennium Science Initiative through grant IC 120009, awarded to the Millennium Institute of Astrophysics (MAS); and by Proyecto Basal AFB-170002. I.D. and E.K.G. were supported by Sonderforschungsbereich SFB 881 “The Milky Way System” (subproject A03) of the German Research Foundation (DFG).

References

- Alonso-García, J., Dékány, I., Catelan, M., et al.: Variable Stars in the VVV Globular Clusters. I. 2MASS-GC 02 and Terzan 10. *The Astronomical Journal* 149, 99 (2015)
- Alonso-García, J., Saito, R. K., Hempel, M., et al.: Milky Way demographics with the VVV survey. IV. PSF photometry from almost one billion stars in the Galactic bulge and adjacent southern disk. *Astronomy & Astrophysics* 619, A4 (2018)
- Bonifacio, P., Monai, S., Beers, T. C.: A Search for Stars of Very Low Metal Abundance. V. Photoelectric UB_V Photometry of Metal-weak Candidates from the Northern HK Survey. *The Astronomical Journal* 120, 2065–2081 (2000)
- Borissova, J., Bonatto, C., Kurtev, R., et al.: New Galactic star clusters discovered in the VVV survey. *Astronomy & Astrophysics* 532, A131 (2011)
- Braga, V. F., Contreras Ramos, R., Minniti, D., et al.: New type II Cepheids from VVV data towards the Galactic center. *arXiv:1904.12024* (2019)
- Casali, M., Adamson, A., Alves de Oliveira, C., et al.: The UKIRT wide-field camera. *Astronomy & Astrophysics* 467, 777–784 (2007)
- Cioni, M.-R. L., Clementini, G., Girardi, L., et al.: The VMC survey. I. Strategy and first data. *Astronomy & Astrophysics* 527, A116 (2011)
- Chené, A.-N., Borissova, J., Clarke, J. R. A., et al.: Massive open star clusters using the VVV survey. I. Presentation of the data and description of the approach. *Astronomy & Astrophysics* 545, A54 (2012)
- Cross, N. J. G., Collins, R. S., Mann, R. G., et al.: The VISTA Science Archive. 548, A119 (2012)
- Contreras Ramos, R., Minniti, D., Gran, F., et al.: The VVV Survey RR Lyrae Population in the Galactic Center Region. *The Astrophysical Journal* 863, 79 (2018)
- Dékány, I., Minniti, D., Catelan, M., et al.: VVV Survey Near-infrared Photometry of Known Bulge RR Lyrae Stars: The Distance to the Galactic Center and Absence of a Barred Distribution of the Metal-poor Population. *The Astrophysical Journal*, 776, L19 (2013)

- Dékány, I., Hajdu, G., Grebel, E. K., et al.: A Near-infrared RR Lyrae Census along the Southern Galactic Plane: The Milky Way's Stellar Fossil Brought to Light. *The Astrophysical Journal* 857, 54 (2018)
- Emerson, J. P., Irwin, M. J., Lewis, J., et al.: VISTA data flow system: overview. *Proceedings of SPIE* 5493, 401 (2004)
- Gonzalez, O. A., Rejkuba, M., Zoccali, M., et al.: Reddening and metallicity maps of the Milky Way bulge from VVV and 2MASS. II. The complete high resolution extinction map and implications for Galactic bulge studies. *Astronomy & Astrophysics* 543, A13. (2012)
- González-Fernández, C., Hodgkin, S. T., Irwin, M. J., et al.: The VISTA ZYJHKs photometric system: calibration from 2MASS. *Monthly Notices of the Royal Astronomical Society* 474, 5459–5478 (2018)
- Hajdu, G., Dékány, I., Catelan, M., Grebel, E. K., Jurcsik, J.: A Data-driven Study of RR Lyrae Near-IR Light Curves: Principal Component Analysis, Robust Fits, and Metallicity Estimates. *The Astrophysical Journal* 857, 55 (2018)
- Hodgkin, S. T., Irwin, M. J., Hewett, P. C., Warren, S. J.: The UKIRT wide field camera ZYJHK photometric system: calibration from 2MASS. *Monthly Notices of the Royal Astronomical Society* 394, 675–692 (2009)
- Irwin, M. J., Lewis, J., Hodgkin, S., et al.: VISTA data flow system: pipeline processing for WFCAM and VISTA. *Proceedings of SPIE* 5493, 411–422 (2004)
- Magnier, E. A., Schlafly, E., Finkbeiner, D., et al.: The Pan-STARRS 1 Photometric Reference Ladder, Release 12.01. *The Astrophysical Journal Supplement* 205, 20 (2013)
- Minniti, D., Lucas, P. W., Emerson, J. P., et al.: VISTA Variables in the Vía Láctea (VVV): The public ESO near-IR variability survey of the Milky Way. *New Astronomy* 15, 433–443 (2010)
- Minniti, D. 2018, The Vatican Observatory, Castel Gandolfo: 80th Anniversary Celebration, 51, 63
- Nataf, D. M., Gonzalez, O. A., Casagrande, L., et al.: Interstellar extinction curve variations towards the inner Milky Way: a challenge to observational cosmology. *Monthly Notices of the Royal Astronomical Society* 456, 2692–2706 (2016)
- Jurcsik, J., Hajdu, G., Dékány, I., et al., Blazhko modulation in the infrared. *Monthly Notices of the Royal Astronomical Society* 475, 4208–4222 (2018)
- Schlafly, E. F., Finkbeiner, D. P., Jurić, M., et al.: Photometric Calibration of the First 1.5 Years of the Pan-STARRS1 Survey. *The Astrophysical Journal* 756, 158 (2012)
- Schlegel, D. J., Finkbeiner, D. P., Davis, M.: Maps of Dust Infrared Emission for Use in Estimation of Reddening and Cosmic Microwave Background Radiation Foregrounds. *The Astrophysical Journal* 500, 525–553 (1998)
- Schultheis, M., Chen, B. Q., Jiang, B. W., et al.: Mapping the Milky Way bulge at high resolution: the 3D dust extinction, CO, and X factor maps. *Astronomy & Astrophysics* 566, A120 (2014)

- Skrutskie, M. F., Cutri, R. M., Stiening, R., et al.: The Two Micron All Sky Survey (2MASS). *The Astronomical Journal* 131, 1163–1183 (2006)
- Sutherland, W., Emerson, J., Dalton, G., et al.: The Visible and Infrared Survey Telescope for Astronomy (VISTA): Design, technical overview, and performance. *Astronomy & Astrophysics* 575, A25 (2015)
- Wegg, C., & Gerhard, O.: Mapping the three-dimensional density of the Galactic bulge with VVV red clump stars. *Monthly Notices of the Royal Astronomical Society* 435, 1874–1887 (2013)